Real-Space Transfer and Trapping of Carriers into Single GaAs Quantum Wires Studied by Near-Field Optical Spectroscopy

A. Richter, G. Behme, M. Süptitz, Ch. Lienau, and T. Elsaesser
Max-Born-Institut für Nichtlineare Optik und Kurzzeitspektroskopie, D-12489 Berlin, Germany

M. Ramsteiner, R. Nötzel, and K. H. Ploog
Paul-Drude-Institut für Festkörperelektronik, D-10117 Berlin, Germany
(Received 18 February 1997)

We report the first near-field optical study of *single* GaAs quantum wires grown on patterned (311)*A* GaAs surfaces. Spatially resolved optical spectra at a temperature of 10 K give evidence for one-dimensional carrier confinement and subband structure. At 300 K, electron-hole pairs in continuum states undergo diffusive real-space transfer over a length of several microns determined by hole mobility and trapping by optical phonon emission. Optical phonon scattering of carriers in the quantum wire establishes a quasiequilibrium carrier distribution in both wire and continuum states. [S0031-9007(97)03977-X]

PACS numbers: 78.66.Fd, 78.55.Cr

Optical and transport properties of semiconductor nanostructures have attracted substantial interest as tailoring the dimensions and/or composition of such materials leads to new physical properties and optimized performance of devices. Quasi-two-dimensional (2D) quantum wells (QW) and superlattices have been investigated in great detail whereas quasi-one-dimensional (1D) structures of high structural quality became available only recently. Such quantum wire (QWR) systems were realized by photolithography and deep mesa etching of QWs [1], epitaxial growth on tilted [2] or prestructured [3] substrates, or by cleaved-edge QW overgrowth [4].

The optical properties and the microscopic carrier dynamics of quantum wires have mainly been studied with ensembles consisting of up to hundreds of nanostructures, due to the limited spatial resolution of the optical techniques applied. In such experiments, size fluctuations within the ensemble of nanostructures lead to an additional inhomogeneous broadening of the optical spectra, frequently making the observation of the intrinsic 1D behavior difficult. Furthermore, processes involving real-space transfer of carriers are difficult to separate from carrier relaxation in the QWR. This is particularly relevant for carrier capture into a QWR where—in general—both real-space transfer in delocalized states and trapping at the QWR location occur [5–7]. Until now, a clear separation of such processes, which is essential for understanding the underlying physics, has not been possible.

Experimental techniques with a spatial resolution in the submicron range have the potential to study *single* nanostructures and, thus, to spatially separate the different microscopic processes. Both cathodoluminescence [5,6] and near-field scanning optical microscopy (NSOM) [8,9] have been applied to investigate single quantum wires, in the case of NSOM with energetically well-defined excitation. In this Letter, we present the first near-field optical study of real-space transfer and capture of carriers into a single GaAs quantum wire. Steady-state and time-resolved photoluminescence (PL) and photoluminescence excitation (PLE) measurements based on NSOM were performed with a novel type of GaAs QWR. We demonstrate that the transfer of carriers from 2D continuum states into the QWR involves (i) real-space transfer of electron-hole pairs over characteristic lengths of several microns with a diffusion coefficient determined by hole mobility, and (ii) carrier trapping by emission of optical phonons. At room temperature, carrier-optical phonon scattering establishes a quasiequilibrium carrier distribution populating both 1D QWR and 2D QW states.

The QWR structure investigated in our experiments is depicted schematically in Fig. 1 [10,11]. The sample was grown by molecular beam epitaxy on patterned GaAs (311)*A* substrates at the sidewall of 15–20 nm high mesa stripes oriented along [01-1]. The sample consists of a nominally 6 nm thick GaAs QW layer clad by 50 nm thick $Al_{0.5}Ga_{0.5}As$ barriers. In the growth process, formation of a sidewall QWR arises from the preferential migration of Ga atoms within the QW layer from the mesa top and the mesa bottom towards the sidewall [10]. Cross sectional TEM images indicate that the thickness of the GaAs QW at the sidewall increases up to 13 nm, resulting in a 1D confinement over a lateral width of 50 nm. Measurements of the diamagnetic shift of the PL energy confirm the 1D quantum confinement [11].

A novel near-field scanning optical microscope for sample temperatures between 10 and 300 K [12] was used to record optical spectra of a single QWR. A spatial resolution of better than 200 nm is provided by the nanometer sized aperture of a fiber tip. In the illumination mode, the sample was excited through the fiber tip and PL was recorded through a conventional microscope lens. In the collection mode, we applied broad area excitation

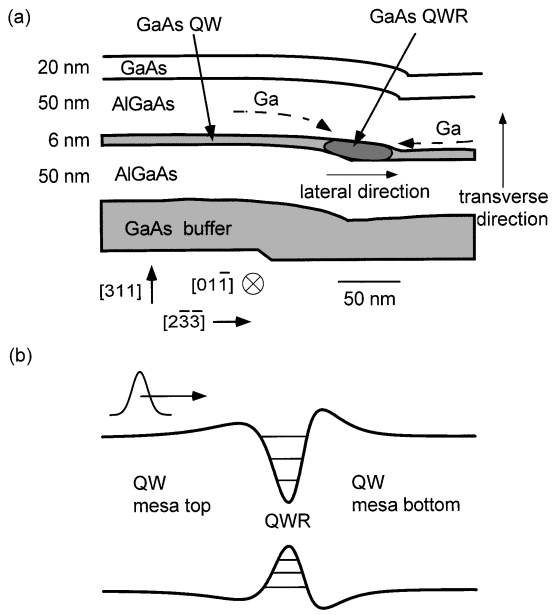

FIG. 1. (a) Schematic of the quantum wire structure. The one-dimensional confinement originates from the thickness variation of the GaAs quantum well along the lateral direction. (b) Schematic energy diagram: potential energy and subband structure along the lateral direction. Diffusion of carriers locally excited in the quantum well is depicted schematically.

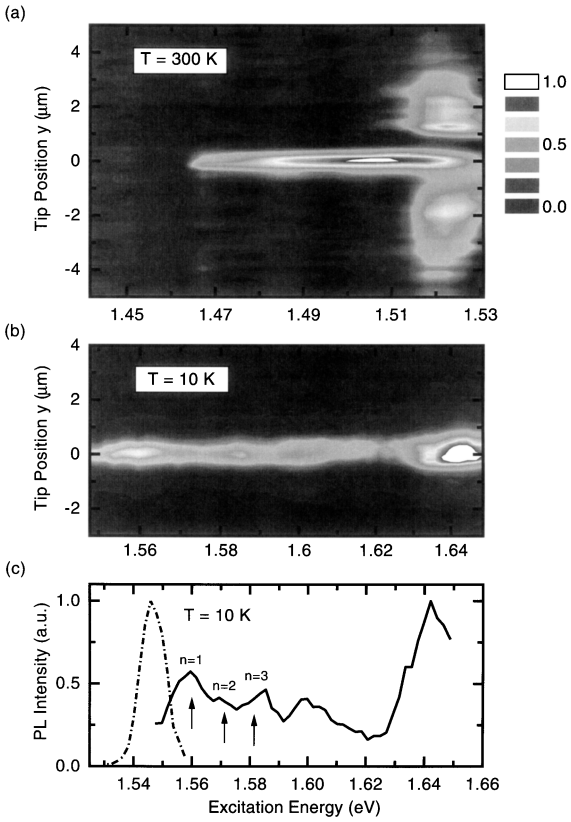

FIG. 2. Near-field PLE spectra of the QWR sample for local excitation through the fiber tip. The intensity of QWR luminescence is plotted as a function of excitation energy (abscissa) and of lateral distance between the QWR located at $y = 0$ and the fiber tip (ordinate). (a) Sample temperature 300 K, detection energy 1.459 eV. For excitation below 1.515 eV, electron-hole pairs are excited exclusively in the QWR. Above 1.515 eV, carriers excited in the QW contribute to the PL signal. (b) Sample temperature 10 K, detection energy 1.544 eV. Only carriers excited at the QWR contribute to the signal. (c) Cross section through (b) at $y = 0$ (solid line) and luminescence spectrum (dash-dotted line).

through a lens (spot size 30 μm) and detected the emitted light through the fiber tip. Spatially resolved images were recorded by scanning the sample relative to the probe tip [8,12]. The PL dispersed in a double monochromator (resolution 1 nm) was detected with a silicon avalanche photodiode, either in steady state or with a time resolution of 250 ps. Different tunable lasers served for steady state and/or time-resolved excitation of the sample with powers between 10 and 100 nW, corresponding to a very low carrier density between 10^4 and 10^5 cm^{-1}.

In Figs. 2(a) and 2(b) we present spatially resolved PLE spectra of a single QWR at 300 and 10 K, respectively. The PL intensity is plotted as a function of excitation energy E_{ex} and of the lateral separation between the excitation tip and the QWR located at $y = 0$. At 300 K, photoexcitation at $E_{ex} < 1.515$ eV occurs exclusively in a narrow region along $y = 0$. The width of this area (FWHM) has a value of 260 nm and is limited by the specific sample structure as will be discussed elsewhere. At photon energies $E_{ex} > 1.515$ eV, QWR luminescence is observed even for a finite lateral distance of the excitation tip from the QWR, i.e., for excitation of the QW, giving rise to the bright areas at positive and negative y values in Fig. 2(a).

In contrast, the low-temperature data in Fig. 2(b) show luminescence exclusively for excitation at the QWR. The cross section through this image [Fig. 2(c), solid line] exhibits several maxima below the onset of QW absorption. Such peaks are due to the quasi-1D subband structure of the QWR. Preliminary calculations of the optical transition energies suggest that the first three peaks are due to the $n = 1$, $n = 2$, and $n = 3$ heavy hole to conduction band transitions [arrows in Fig. 2(c)] [13]. From the separation between the first peak and the onset of QW absorption, one derives a confinement energy of about 80 meV. The small Stokes shift of 10 meV between the first peak and the PL maximum and the narrow PL spectrum (dash-dotted line) indicate the high structural quality of the sample. The small inhomogeneous broadening in the spectra is—most probably—related to exciton localization induced by interface roughness on a length scale between the exciton diameter and the spatial resolution of 250 nm.

In Fig. 3 the PL intensity at 300 K is plotted logarithmically versus the lateral distance of the exciting fiber tip from the QWR (excitation energy 2 eV). Because of

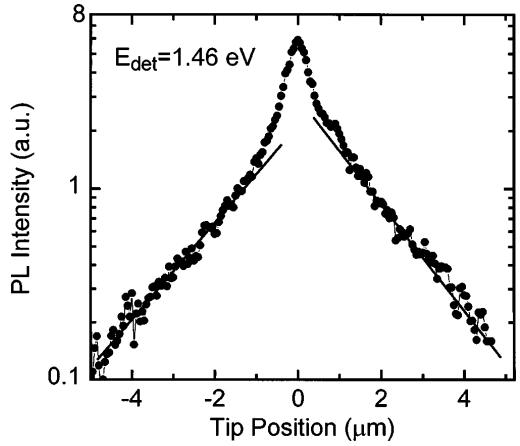

FIG. 3. Spatial profile of QWR luminescence at 300 K. The PL intensity at 1.46 eV is plotted logarithmically versus the separation of the excitation tip from the QWR (excitation at 2 eV).

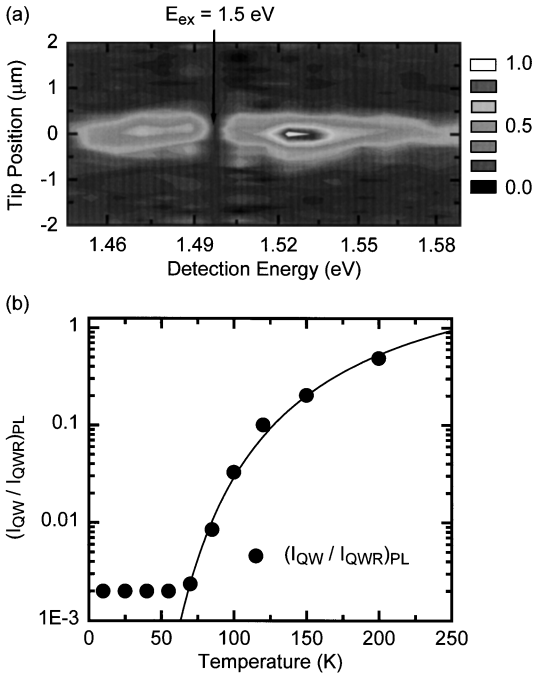

FIG. 4. (a) Near-field PL spectrum for resonant spatially resolved QWR excitation at 1.5 eV. The PL signal at room temperature is plotted as a function of detection energy and lateral separation of QWR and excitation tip. Note the strong QW emission at photon energies higher than the excitation. (b) Ratio of QW to QWR luminescence intensity as a function of sample temperature (logarithmic ordinate scale). Solid line: Intensity ratio calculated with an activation energy of 45 meV for carrier transfer from the QWR to the QW.

the high dynamic range of this measurement, the monoexponential decrease of PL at positive and negative tip positions is clearly resolved and extends over a length of several microns. The occurrence of QWR luminescence after QW excitation involves carrier diffusion and trapping, i.e., a collection of carriers in the QWR, as will be discussed in detail below. To get a more specific insight into carrier exchange between the QWR and the QW, measurements with resonant excitation of the QWR were performed. In Fig. 4(a) a luminescence image is shown which was recorded at 300 K with localized excitation at 1.5 eV. In addition to the QWR luminescence between 1.45 and 1.50 eV, intense emission is found at the spectral position of QW luminescence, i.e., at photon energies higher than the excitation energy. Measurements with spatially resolved detection show indeed that it originates from carriers transferred from the QWR to the QW [13]. The energy excess of the emitted photons with respect to the excitation is provided by inelastic scattering processes in the sample. The activation energy of the QW emission was derived from the intensity ratio of QW to QWR luminescence measured at different temperatures [Fig. 4(b), symbols]. The strong increase of QW emission with temperature is reproduced by a simple numerical analysis assuming a Boltzmann distribution for the QWR and the QW carrier distributions and an activation energy of 45 meV (solid line). Time resolved measurements of QWR and QW PL at 300 K give monoexponential decays of PL intensity with time constants of 1.9 and 2.1 ns, respectively. The QW lifetime was measured with excitation far from the QWR to suppress the influence of carrier trapping on the kinetics.

We now discuss the microscopic processes of carrier transfer from the 2D continuum into the QWR and vice versa. The data taken at 300 K allow a clear separation of the two relevant phenomena, namely, real-space transfer of electron-hole pairs to the QWR and trapping into the 1D subband system [Fig. 1(b)]. The PLE data (Figs. 2 and 3) show that carriers generated by localized excitation of the QW undergo diffusive transport over a length of up to several microns until they are trapped and contribute to QWR emission. The diffusion length L_d is determined by the recombination lifetime $\tau_{\mathrm{rec}} = 2.1$ ns of the 2D carriers and the ambipolar diffusion coefficient D. Correspondingly, the PL signal $I_{\mathrm{QWR}}(y)$ is expected to decrease exponentially with increasing distance from the QWR, i.e., $I_{\mathrm{QWR}}(y) \propto \exp(-|y|/L_d)$. For a tip separation $|y| > 1$ μm, the data in Fig. 3 exhibit exactly this behavior giving a value of $L_d = 1.6$ μm. Using $D = (L_d)^2/\tau_{\mathrm{rec}}$ and $\mu_{\mathrm{eff}} = De/(kT)$ for the effective mobility of the carriers (e, electron charge, kT, thermal energy), one derives values of $D = 12.2$ cm^2/s and $\mu_{\mathrm{eff}} = 488$ cm^2/V s at $T = 300$ K. This μ_{eff} is close to the mobility of holes in GaAs at 300 K [14], whereas electron mobilities are much higher. We conclude that hole diffusion determines the real-space transfer.

A comment should be made on the change of the spatial PLE profiles with excitation energy E_{ex} and temperature. For photon energies at the onset of the QW absorption at 300 K ($E_{\mathrm{ex}} = 1.52$ eV), Fig. 2(a) displays narrow dark

areas in the vicinity of the QWR, i.e., a local decrease of the PL signal. This is due to local changes of the interband transition energy in our sample. In particular, the formation of the QWR by Ga atom migration in the growth process results in a thinning of the GaAs QW in the vicinity of the QWR and a blueshift of the local QW interband absorption [Fig. 1(b)]. As a result, the QW absorption at 1.52 eV and the PL signal are reduced. In contrast, the spatially more or less constant excitation at a higher photon energy $E_{ex} = 2$ eV (Fig. 3) results in an exponential profile of the signal extending to smaller separations from the QWR. The peak at $y = 0$ in Fig. 3 is due to direct excitation of carriers at the location of the QWR. For carrier transport, the band gap increase close to the QWR represents a local barrier. At 300 K carriers diffusing to the QWR can move through this area because of their relatively large thermal energy ($kT = 25$ meV). At 10 K, however, transport through this region is suppressed as is evident from the spatially confined image in Fig. 2(b).

In addition to real-space transfer, carrier trapping into the QWR and the reverse process of carrier excitation from the QWR into the QW continuum determine the optical spectra at 300 K. Both QW and QWR luminescence are observed after excitation in the QW continuum (Figs. 2 and 3) [13] and after localized excitation of the QWR (Fig. 4). The shape of such emission bands is very close to the spectra found with resonant excitation. This shows that a quasiequilibrium carrier distribution populating both the 2D continuum and the 1D subband system is formed within the nanosecond QW and QWR recombination lifetimes.

In general, carrier exchange between 1D and 2D states and equilibration of the carrier distribution involve carrier-carrier and carrier-phonon scattering, both occurring on femto- to picosecond time scales, much faster than the nanosecond recombination times. Furthermore, the cooling of carriers excited at 2 eV (Fig. 3) down to 300 K proceeds in the picosecond regime. In our experiments, the very low carrier density ($<10^5$ cm^{-1}) is equivalent to a situation where—on the average—a single electron-hole pair populates the QWR within the recombination lifetime. Thus, the relaxation scenario is governed by scattering with optical and acoustic phonons, whereas carrier-carrier scattering and Auger processes play a minor role. For trapping into the QWR, theoretical calculations suggest scattering rates with optical phonons in the order of several 10^{12} s^{-1}, at least 10 times higher than with acoustic phonons [7,15,16]. The inverse promotion process of confined QWR carriers into the QW is thermally activated with an activation energy of 45 meV, essentially determined by the (electron) confinement energy of about 60 meV. Here absorption of single optical phonons represents the dominant mechanism whereas multiple absorption of acoustic phonons is much less important.

In summary, we studied the nanoscopic optical properties of a novel quantum well embedded QWR structure. The high spatial resolution of the NSOM technique allowed us to separate the optical spectra of QWR and QW and provides evidence for a quasi-one-dimensional carrier confinement. Real-space transfer and capture of carriers into the QWR are separately resolved. At elevated temperatures, we observe carrier excitation from QWR into QW states by optical phonon absorption. Our experiments demonstrate that time- and spatially resolved near-field microscopy in a broad temperature range opens up a new avenue towards the understanding of transport and capture processes in low-dimensional semiconductors.

[1] T. Demel, D. Heitmann, P. Grambow, and K. Ploog, Phys. Rev. Lett. **66**, 2657 (1991).

[2] M. Tsuchiya, J. M. Gaines, R. H. Yan, R. J. Simes, P. O. Holtz, L. A. Coldren, and P. M. Petroff, Phys. Rev. Lett. **62**, 466 (1989).

[3] E. Kapon, D. M. Hwang, and R. Bhat, Phys. Rev. Lett. **63**, 430 (1989).

[4] A. R. Goni, L. N. Pfeiffer, K. W. West, A. Pinczuk, H. U. Baranger, and H. L. Störmer, Appl. Phys. Lett. **61**, 1956 (1992).

[5] M. Walther, E. Kapon, J. Christen, D. M. Hwang, and R. Bhat, Appl. Phys. Lett. **60**, 521 (1992).

[6] M. Grundmann *et al.*, Semicond. Sci. Technol. **9**, 1939 (1994).

[7] J. F. Ryan *et al.*, Phys. Rev. B **53**, R4225 (1996).

[8] E. Betzig, P. L. Finn, and J. S. Weiner, Appl. Phys. Lett. **60**, 2484 (1992).

[9] T. D. Harris *et al.*, Appl. Phys. Lett. **68**, 988 (1996).

[10] R. Nötzel, M. Ramsteiner, J. Menniger, A. Trampert, H.-P. Schönherr, L. Däweritz, and K. H. Ploog, Jpn. J. Appl. Phys. **35**, L297 (1996).

[11] R. Nötzel *et al.*, J. Appl. Phys. **80**, 4108 (1996).

[12] G. Behme, A. Richter, M. Süptitz, and C. Lienau (to be published).

[13] A. Richter *et al.* (unpublished).

[14] D. C. Look *et al.*, in *Properties of GaAs* (INSPEC, London, 1990), p. 97.

[15] N. Nishiguchi, Phys. Rev. B **54**, 9819 (1996).

[16] L. Rota, F. Rossi, P. Lugli, and E. Molinari, Phys. Rev. B **52**, 5183 (1995).